

THE LIGHT ECHO AROUND SUPERNOVA 2003GD IN MESSIER 74¹

SCHUYLER D. VAN DYK

Spitzer Science Center, Caltech, Mailcode 220-6, Pasadena CA 91125

WEIDONG LI AND ALEXEI V. FILIPPENKO

Department of Astronomy, 601 Campbell Hall, University of California, Berkeley, CA 94720-3411

To appear in PASP, 2006 March

ABSTRACT

We confirm the discovery of a light echo around the Type II-plateau Supernova 2003gd in Messier 74 (NGC 628), seen in images obtained with the High Resolution Channel of the Advanced Camera for Surveys on-board the *Hubble Space Telescope* (*HST*), as part of a larger Snapshot program on the late-time emission from supernovae. The analysis of the echo we present suggests that it is due to the SN light pulse scattered by a sheet of dust grains located ~ 113 pc in front of the SN, and that these grains are not unlike those assumed to be in the diffuse Galactic interstellar medium, both in composition and in size distribution. The echo is less consistent with scattering off carbon-rich grains, and, if anything, the grains may be somewhat more silicate-rich than the Galactic dust composition. The echo also appears to be more consistent with a SN distance closer to 7 Mpc than 9 Mpc. This further supports the conclusion we reached elsewhere that the initial mass for the SN progenitor was relatively low ($\sim 8\text{--}9 M_{\odot}$). *HST* should be used to continue to monitor the echo in several bands, particularly in the blue, to better constrain its origin.

Subject headings: (stars:) supernovae: general — (stars:) supernovae: individual (SN 2003gd) — (ISM:) reflection nebulae — (ISM:) dust, extinction — galaxies: individual (Messier 74, NGC 628)

1. INTRODUCTION

The scattering of supernova (SN) light by dust nearby to the event in the host galaxy is likely a common occurrence. The presence of light echoes around supernovae (SNe) has been inferred based on infrared excesses (e.g., Dwek 1983; Graham et al. 1983; Graham & Meikle 1986). However, up until recently, only five SNe have had echoes unambiguously discovered around them: SN 1987A in the Large Magellanic Cloud, SN 1991T in NGC 4527, SN 1993J in Messier 81 (M81), SN 1998bu in Messier 96 (M96), and SN 1999ev in NGC 4274 (Maund & Smartt 2005). In the cases of the Type Ia SNe 1991T (Schmidt et al. 1994) and 1998bu (Cappellaro et al. 2001), indications of a light echo were evident in the ground-based, late-time optical observations. However, it required the superior angular resolution of the *Hubble Space Telescope* (*HST*) to visually confirm for both SNe the existence of the echoes (Sparks et al. 1999; Cappellaro et al. 2001). Although for the Type II SN 1987A the interstellar (e.g., Crotts 1988) and circumstellar (e.g., Emmering & Chevalier 1989; Bond et al. 1990) echoes could be discovered from the ground, for the Type IIb SN 1993J the discovery of echoes (Sugerman & Crotts 2002; Liu, Bregman, & Seitzer 2003) again is a result of the high-resolution imaging capabilities of *HST*.

These light echoes result as the luminous ultraviolet (UV)/optical emission pulse from a SN is scattered by dust in dense regions of the SN environment. The UV pulse will tend to photoionize the circumstellar matter and destroy smaller dust grains nearest to the SN, while more distant, larger grains survive the pulse; SNe therefore have the potential to illuminate the most distant interstellar material and the largest structures in the environment (Sugerman

2003). We observe the echo as a ring, or arc, but it is actually an ellipsoid with the SN and the observer at the foci and defined by the light travel time from the SN (see, e.g., Fig. 1 in Patat 2005). Light echoes provide a means to probe both the circumstellar and interstellar structures around SNe. With a precise distance to the SN and the observed geometry of the echo, we can accurately determine the three-dimensional distribution of dust in the SN environment.

Conversely, as was elegantly shown by Panagia et al. (1991) in the case of SN 1987A, light echoes around a SN provide a means to measure the distance to the SN, based purely on geometrical arguments and independent of any distance ladder. The polarized light from the dust echo may facilitate this distance determination (Sparks 1994, 1996). Finally, knowing the SN spectrum, which is what is scattered by the dust echo, we can determine the size distribution and composition of the dust (e.g., Sugerman 2003).

Sugerman (2005) has recently discovered and analyzed a light echo around the Type II-plateau (II-P) SN 2003gd in Messier 74 (M74), seen in *HST* images we obtained when the SN was appreciably fainter. Here we confirm the discovery of the echo and provide a different analysis.

SN 2003gd was discovered by Evans (2003) on 2003 June 12.82 (UT dates are used throughout this paper) and, based on the light-curve plateau, Van Dyk, Li, & Filippenko (2003) estimate the explosion date at about 2003 March 17. SN 2003gd is a somewhat unusual SN II-P and was recently discussed in detail by Hendry et al. (2005). Of notable interest is that both Van Dyk et al. (2003) and Smartt et al. (2004) independently determined, us-

¹BASED IN PART ON OBSERVATIONS WITH THE NASA/ESA HUBBLE SPACE TELESCOPE, OBTAINED AT THE SPACE TELESCOPE SCIENCE INSTITUTE (STSCI), WHICH IS OPERATED BY AURA, INC., UNDER NASA CONTRACT NAS5-26555.

ing a combination of pre-SN *HST* and ground-based images, that the progenitor was a $\sim 8 M_{\odot}$ red supergiant (RSG), at the lower mass limit of theoretical predictions for core-collapse SNe. The confirmation of the progenitor star was based on late-time *HST* images obtained by Smartt et al. (2004) at age ~ 137 d, when the SN was slightly off the plateau, but still quite bright in the images (see also Hendry et al. 2005).

2. OBSERVATIONS

In Van Dyk et al. (2003) we presented the early-time *BVRI* light curves for SN 2003gd, based on monitoring with the Katzman Automatic Imaging Telescope (KAIT). We have continued monitoring the SN with KAIT and therefore update the ground-based light curves in Table 1. We also list the *BR* late-time magnitudes from our ACS Snapshot images in Table 1. Additionally, we have attempted to measure the SN brightness in the ACS/HRC images obtained by Smartt et al. (2004) on 2003 Aug. 1; the SN is hopelessly saturated in their F814W image, but we are able to measure F435W and F555W magnitudes for the SN through a $0''.5$ -radius aperture. We include these magnitudes, after correction and photometric transformation, in Table 1.

We observed SN 2003gd on 2004 December 8 with the Advanced Camera for Surveys (ACS) High Resolution Channel (HRC) as part of our larger Cycle 13 Snapshot program on the late-time emission from SNe (GO-10272; PI: Filippenko). These images were obtained when the SN was at an age ~ 632 d (1.73 yr), at significantly later times than the Smartt et al. (2004) images. The bandpasses and exposure times we used were F435W (840 s) and F625W (360 s). All of the data for this program have no proprietary period, and thus we obtained these data from the *HST* public archive, where standard pipeline procedures had been employed to calibrate the images.

Unfortunately, in the F435W image a cosmic-ray hit or hot pixel sits directly along the echo due west of the SN, such that the standard pipeline was unable to reject this pixel from the combination of the cosmic-ray split observations. We used the IRAF² tasks “fixpix” and “epix” to interpolate the affected pixel as well as we could. In Figure 1 we show the corrected F435W ($\sim B$) image and the F625W ($\sim R$) image. Although at a relatively low signal-to-noise ratio, the light echo can be readily seen in the *HST* images. (The echo was not detectable in the earlier images by Smartt et al. or in the pre-SN *HST* images.) The relatively bright object within the echo is SN 2003gd.

We measured the SN brightness in both bands, first with a $0''.5$ -radius aperture and then via point-spread function (PSF) fitting (with an equivalent aperture also of $0''.5$ radius). The model PSFs were constructed from two isolated stars in the ACS/HRC images. What is most notable is that the aperture magnitudes for the SN are brighter than the PSF magnitudes, almost certainly because of contamination in the aperture by the echo itself. We adjust the PSF magnitudes to infinite aperture, using the corrections for the HRC in Sirianni et al. (2005), and find $m_{F435W} = 23.76 \pm 0.07$ and $m_{F625W} = 22.96 \pm 0.05$ mag. Using the photometric transformations also in Sirianni et

al., we derive $B = 23.73 \pm 0.08$ and $R = 22.90 \pm 0.05$ mag (Table 1). We caution that these transformations are derived from stars with normal photospheres and not for emission, reflected or otherwise, from sources with unusual spectra, such as SNe. The uncertainties in B and R given here are strictly those in the photometric measurements and in the transformation coefficients, and likely underestimate the actual uncertainties.

The light echo has an asymmetric structure: Only an arc of emission, most noticeably to the northwest, not a complete ring, is seen in both the F435W and F625W bands. Some far weaker emission is seen to the south of the SN; the emission to the east is not part of the echo, but instead are the stars C and D noted by Smartt et al. (2004). After all the stars, including the SN, were subtracted using the model PSFs from the images, the surface brightness of the echo was measured in both bands. We used the IRAF task “minstatistics” with an arc-shaped pixel mask to determine the average count rate per pixel in the echo, i.e., $0.024 \pm 0.013 \text{ s}^{-1} \text{ pixel}^{-1}$ over 82 pixels in F435W and $0.032 \pm 0.021 \text{ s}^{-1} \text{ pixel}^{-1}$ over 78 pixels in F625W. After subtracting the average sky pixel count rate, and with the zero points from Sirianni et al. (2005) and a HRC plate scale of $0''.027 \text{ pixel}^{-1}$, these translate to average surface brightnesses of $\langle \mu_{F435W} \rangle = 21.5 \pm 0.5$ and $\langle \mu_{F625W} \rangle = 21.1 \pm 0.6 \text{ mag arcsec}^{-2}$. Integrating over the echo in each band we derive $m_{F435W} = 24.5 \pm 0.5$ and $m_{F625W} = 24.2 \pm 0.6$ mag, with negligible change in the transformation (again following Sirianni et al.) to $m_B = 24.5 \pm 0.5$ and $m_R = 24.2 \pm 0.6$ mag, given the echo’s color, i.e., $B - R = 0.3 \pm 0.8$ mag. Assuming Vega as photometric zero point, the echo has fluxes $1.1 \pm 0.7 \times 10^{-18}$ and $4.9 \pm 2.8 \times 10^{-19} \text{ erg cm}^{-2} \text{ s}^{-1} \text{ \AA}^{-1}$ at B and R , respectively (Table 2). Note that Sugerman (2005) finds somewhat different values for both the surface brightness ($\mu_{F435W} = 20.8 \pm 0.2$ and $\mu_{F625W} = 21.4 \pm 0.3 \text{ mag arcsec}^{-2}$) and flux ($m_B = 24.2 \pm 0.1$ and $m_R = 23.9 \pm 0.1$ mag), although these values agree with ours to within the uncertainties. The larger uncertainties we estimated for the fluxes, relative to those estimated by Sugerman (2005), arise from the standard deviation in the count rate statistics within the pixel mask. Given the low signal-to-noise ratio of the echo in the images in both bands, we consider our uncertainties to be quite conservative.

3. ANALYSIS

Here we provide an analysis of the echo and its origin. We note that this analysis differs from that presented by Sugerman (2005). We have determined that SN 2003gd is at the exact center of the light echo, with uncertainty $< 0.2 \text{ pixel}$ ($< 0''.005$), through comparison of our Snapshot images to the ACS F435W images obtained by Smartt et al. (2004), when the SN was significantly brighter. The SN itself therefore must be the source of the echo, which we observe at age t after explosion and age τ after optical maximum. The observed echo is the product of the input SN pulse and scattering by dust in the environment.

Following Liu et al. (2003) and Schaefer (1987), we can approximate the ellipsoid near the SN as a paraboloid. The perpendicular linear distance of the line-of-sight to the

²IRAF (Image Reduction and Analysis Facility) is distributed by the National Optical Astronomy Observatories, which are operated by the Association of Universities for Research in Astronomy, Inc., under cooperative agreement with the National Science Foundation.

SN from the line-of-sight to the echo, the so-called “impact parameter,” is $b = D\theta$, where D is the SN’s distance from Earth and θ is the angular distance of the two lines-of-sight. We measure a radius for the echo of 11.5 ± 1.0 pixel which then corresponds to $\theta = 0''.31 \pm 0''.03$. For the SN distance we assume $d = 7.2$ Mpc (Van Dyk et al. 2003), $b = 10.8 \pm 1.1$ pc. We note that Smartt et al. (2004) assume a SN distance of 9.1 Mpc and Hendry et al. (2005) have estimated a distance of 9.3 Mpc. For the latter distance, $b = 14.0 \pm 1.3$ pc (hereafter, we will also provide in parentheses estimates of the various parameters assuming a distance of 9.3 Mpc). The age t , derived from the assumed explosion date, 2003 March 17 (Van Dyk et al. 2003), is 631 d, or 1.73 yr. However, the echo really appears due to the SN pulse, primarily in the UV and the blue; we will assume that the SN 2003gd B light curve is similar to that of SN 1999em (see below), and Leonard et al. (2002) determine that the B maximum for the latter SN occurred about 8 days after explosion. Therefore, $\tau = 623$ d, or 1.71 yr. The distance from the SN to the echo, $r = l + c\tau$, can be derived from $r^2 = b^2 + l^2$. For $c\tau = 0.52$ pc, we find $l = 112.0 \pm 24.0$ pc and $r = 112.5 \pm 23.5$ pc ($l = 188.0 \pm 37.0$ and $r = 188.5 \pm 37.0$ pc for 9.3 Mpc).

Given this distance and the echo’s overall asymmetric structure, the echo is most likely from interstellar, not circumstellar, dust: For a duration of the RSG phase $\sim 10^4$ yr and wind speed ~ 10 km s $^{-1}$, the circumstellar matter would only be ~ 0.1 pc ($0''.09$) in radius. Additionally, much of this dust is likely destroyed by the UV SN pulse (Sugerman 2003). The observed thickness of the echo is ~ 2 pixels, but the stellar image width (FWHM) is larger than this, so that the echo must be barely resolved, if at all. Therefore, any estimate of the dust sheet thickness along the line-of-sight (Liu et al. 2003) must be an upper limit: For the echo, $\Delta\theta$ is then $\gtrsim 0''.05$, or $\Delta b \gtrsim 1.7$ pc ($\gtrsim 2.2$ pc). The dust sheet thickness is then $\Delta l = (b/ct)\Delta b \gtrsim 35$ pc ($\gtrsim 59$ pc).

As is generally done, we assume that the echo arises from single scattering in a thin sheet of dust between us and the SN, and that the sheet thickness is much smaller than the distance between the SN and the sheet. Following the formalism of Chevalier (1986), Cappellaro et al. (2001), and Patat (2005), the flux F at time t from the echo at a given wavelength or bandpass is

$$F_{\text{echo}}(t) = \int_0^t F_{\text{SN}}(t-t')f(t')dt', \quad (1)$$

where $F_{\text{SN}}(t-t')$ is the flux of the SN at time $t-t'$, and $f(t)$ (in units of s $^{-1}$) determines the fraction of light scattered by the echo toward the observer and depends on the echo geometry and the nature of the dust. The total SN light is effectively treated as a short pulse over which the SN flux is constant.

The term $f(t)$ is assumed to have the form

$$f(t) = \frac{cN_H}{r} \int Q_{\text{sca}}(a)\sigma_g(a)\Phi(\alpha,a)\phi(a)da, \quad (2)$$

where N_H is the H number density, $Q_{\text{sca}}(a)$ is the scattering coefficient for a given grain radius a , $\sigma_g(a) = \pi a^2$ is the dust grain cross section for scattering, and $\Phi(\alpha)$ is the phase function (Henry & Greenstein 1941)

$$\Phi(\alpha, a) = \frac{1 - g(a)^2}{4\pi[1 + g(a)^2 - 2g(a)\cos(\alpha)]^{3/2}}, \quad (3)$$

where α is the scattering angle defined by $\cos(\alpha) = [(b/c\tau)^2 - 1]/[(b/c\tau)^2 + 1]$ (e.g., Schaefer 1987). The function $\Phi(\alpha)$ is applicable for the bandpasses being considered here (see Draine 2003). The term $g(a)$ measures the degree of forward scattering for a dust grain of radius a . From the geometric parameters for this echo, the scattering angle is then $\alpha \approx 5:5$ ($4:3$). The term $\phi(a)$ is the grain size distribution for grain radius a . Following Sugerman (2003), we consider the dust grain distributions for (spherical) silicate and carbonaceous grains from Weingartner & Draine (2001), and the $Q_{\text{sca}}(a)$ and $g(a)$ for “smoothed UV astronomical silicate” grains (Draine & Lee 1984; Laor & Draine 1993; Weingartner & Draine 2001) and for carbonaceous graphite (Draine & Lee 1984; Laor & Draine 1993).

To derive the SN fluence we must integrate the light curves over time in each band. Unfortunately, SN 2003gd was caught late in its evolution, ~ 90 d after explosion. In Van Dyk et al. (2003) we showed from the initial ground-based $BVRI$ light curves that the agreement with the light curves in the same bands for the Type II-plateau SN 1999em (Hamuy et al. 2001; Leonard et al. 2002, 2003) is quite good on the plateau. It is after the plateau that SN 2003gd and SN 1999em fail to agree well. This is due to SN 2003gd being among the peculiar, low luminosity, low ^{56}Ni yield, SNe II-P, including also SN 1997D (Turatto et al. 1998; Benetti et al. 2001) and SN 1999br (Zampieri et al. 2003; Pastorello et al. 2004). However, these latter SNe all appear to agree relatively well with SN 1999em near maximum and early on the plateau as well.

In Figure 2 we show a more complete set of light curves in the B and R bands for SN 2003gd, which includes the updated ground-based datapoints and the addition of the *HST* photometry. The SN 2003gd light curves have been adjusted in time to match the SN 1999em light curves; no adjustment in magnitude was necessary. The relatively good match on the plateau phase for both SNe suggests that we can employ the early-time SN 1999em data to extrapolate the SN 2003gd light curves back to the date of explosion. Performing the integration, assuming Vega as the flux zero point, we find 7.26×10^{-8} and 8.85×10^{-8} erg cm $^{-2}$ Å $^{-1}$ in B and R , respectively (note that these differ with the fluences reported by Sugerman 2005, i.e., 8.0×10^{-8} and 7.0×10^{-8} erg cm $^{-2}$ Å $^{-1}$ in B and R , respectively). If the SN 2003gd light curves evolved in a similar manner to SN 1999em at early times, then these fluences (and the color curves for SN 1999em from Leonard et al. 2002) emphasize how red the SN likely became soon after maximum light. That is, the SN pulse resulting in the echo was relatively red in color.

The duration of the SN pulse in each bandpass can be obtained by assuming $F_{\text{SN}}\Delta t_{\text{SN}} = \int_0^\infty F_{\text{SN}}(t)dt$ (Cappellaro et al. 2001; Patat 2005). Here we take F_{SN} to be the SN maximum flux, which we assume to be the B and R maximum fluxes for SN 1999em (Leonard et al. 2002), i.e., $m = 13.79$ and 13.63 mag in B and R , respectively, and Δt_{SN} to be the pulse duration (this is actually what is termed the “effective width” of the pulse). We then find Δt_{SN} to be ~ 45 d in B and ~ 138 d (about three times longer) in R .

We can estimate the H column density from the extinction toward the echo. We assume that, since the echo lies quite close to the line-of-sight to SN 2003gd, the echo suffers the same amount of extinction as does the SN. For the SN we estimate a total reddening $E(B - V) = 0.13 \pm 0.03$ mag (Van Dyk et al. 2003; Smartt et al. 2004 derive a consistent estimate of the SN reddening, but with a larger uncertainty, $E(B - V) = 0.11 \pm 0.16$ mag). Next, we must subtract the Galactic reddening contribution, $E(B - V) = 0.07$ mag (Schlegel, Finkbeiner, & Davis 1998). Assuming the ratio of total-to-selective extinction $R_V = 3.1$ (e.g., Cardelli, Clayton, & Mathis 1989), we find $A_V = 0.19$ mag internal to the host galaxy. Bohlin, Savage, & Drake (1978) found a fairly constant empirical relation over the diffuse interstellar medium in the Galaxy, $N_H = 5.8 \times 10^{21} E(B - V)$, which provides a normalization for the extinction curve $A_V/N_H = 5.3 \times 10^{-22}$ cm² (Weingartner & Draine 2001). From this relation, and including our estimated uncertainty in the reddening, we derive $N_H = 3.5(\pm 1.7) \times 10^{20}$ cm² in the dust sheet.

In Table 2 we present the fluxes F_{echo} in each band for several echo models, for which we have varied the composition of the dust grains. We have calculated the set of models for both our distance assumption and the Hendry et al. (2005) distance estimate. The first model in the set is the diffuse Galactic dust model from Weingartner & Draine (2001) and Draine (2003); it assumes solar abundances with $R_V = 3.1$ and the total C abundance per H nucleon $b_C = 56$ ppm, with comparable contributions of carbonaceous and silicate dust with radii in the range 5.0 Å – 2.0 μm. We also consider models with $R_V = 3.1$ which are either pure silicates or pure carbonaceous grains. Finally, we consider a model with comparable silicate and carbonaceous grain composition, but assuming $R_V = 4.0$. The results are also shown graphically in Figure 3.

The overall agreement of the models and the observations is remarkably good. With the various assumed model inputs, we are reproducing the observed echo reasonably well, and this further implies that the echo likely arises from the diffuse interstellar dust near the SN. The uncertainties in the model fluxes (arising mostly from the uncertainties in the echo geometrical measurements and in our reddening estimate) are rather large, but are comparable to the measurement uncertainties in the observed fluxes. What we notice is that the C+Si model agrees quite well with the observations. The value of R_V (3.0 or 4.1) has little bearing on this agreement. The pure Si-rich dust model is also consistent with the observations; the pure C-rich dust model, less so (although it agrees to within the uncertainties for $d = 7.2$ Mpc). In fact, for the larger assumed SN distance ($d = 9.3$ Mpc), the pure carbonaceous dust model is no longer consistent with the observations at either band and can be ruled out.

We note that the remaining models calculated for the larger SN distance generally tend to underestimate the flux, although taking into account the large uncertainties in both the observed and model fluxes, it is impossible to rule them out entirely. However, we tentatively suggest that the observed echo may indicate that the actual SN distance is closer to the smaller value we assumed in Van Dyk et al. (2003) than the larger one determined by Hendry et al. (2005; and the similarly larger distance as-

sumed by Smartt et al. 2004). This, along with the value of R_V , has implications for the absolute magnitude, and therefore the initial mass, of the SN progenitor. A higher R_V would imply that the progenitor was, at most, ~ 0.1 mag more luminous than what we estimated in Van Dyk et al. However, the larger distance would require the star to be ~ 0.6 mag more luminous, which would increase the mass estimate by $\sim 1 M_\odot$ (i.e., it would imply that the initial mass was closer to $\sim 10 M_\odot$). The relative agreement between the observed echo and the echo models based on the shorter distance reassures us that our low progenitor mass estimate ($\sim 8-9 M_\odot$), although uncomfortably near the theoretical limit for core collapse (Woosley & Weaver 1986), is realistic.

4. CONCLUSIONS

We have confirmed the presence of a scattered light echo around the nearby Type II-plateau SN 2003gd in M74. This discovery could only have been made in images produced with the superior angular resolution of the *HST* ACS/HRC at sufficiently late times for the SN. We conclude that the echo arises from dust in the interstellar SN environment, and our modeling (within the large uncertainties in the observations, which further propagate into the models) suggests that this dust, both in composition and in grain size distribution, is not unlike dust in the diffuse Galactic interstellar medium, although it is also possible the dust could be more silicate-rich than carbon-rich. In fact, our echo models tend to disfavor dust in the SN environment which is more abundant in carbonaceous grains than silicates. (We note that Sugerman 2005 found that the echo may arise from small carbon-rich grains.)

The models are not particularly sensitive to the value of R_V (but we did not compute models with $R_V > 4$). However, models based on the shorter distance to the SN that we assumed in Van Dyk et al. (2003; 7.2 Mpc) appear to be somewhat more consistent with the observed echo than those for the longer distance assumed by Smartt et al. (2004; 9.1 Mpc) and Hendry et al. (2005; 9.3 Mpc), though the uncertainties are large. These latter two factors slightly increase our confidence in the relatively low estimate ($\sim 8-9 M_\odot$) for the initial mass of the SN progenitor we derived in Van Dyk et al.

From N_H and assuming a path length $L = \Delta l \approx 35$ pc for the dust sheet, the H number density would be $n_H \approx 7$ cm⁻³. Combined with the extinction to the SN, this is consistent with the expectation that light echoes likely emerge from regions with $n_H \approx 10$ cm⁻³ and $A_V \lesssim 1$ mag (Sugerman 2003).

This echo should be further monitored with *HST*, including use of additional bands, particularly in the UV, to far better constrain the nature of the scattering dust and the echo geometry, and to reveal further new or evolving structures in the echo.

The work of A.V.F.'s group at UC Berkeley is supported by NSF grant AST-0307894, as well as by NASA grants GO-10272, AR-10297, and AR-10690 from the Space Telescope Science Institute, which is operated by AURA, Inc., under NASA contract NAS5-26555. A.V.F. is also grateful for a Miller Research Professorship at U.C. Berkeley, during which part of this work was completed. KAIT

was made possible by generous donations from Sun Microsystems, Inc., the Hewlett-Packard Company, Auto-Scope Corporation, Lick Observatory, the National Sci-

ence Foundation, the University of California, and the Sylvia & Jim Katzman Foundation. We thank the referee for useful comments.

REFERENCES

- Benetti, S., et al. 2001, MNRAS, 322, 361
 Bohlin, R. C., Savage, B. D., & Drake, J. F. 1978, ApJ, 224, 132
 Bond, H. E., Gilmozzi, R., Meakes, M. G., & Panagia, N. 1990, ApJ, 354, L49
 Cappellaro, E., et al. 2001, ApJ, 549, L215
 Cardelli, J. A., Clayton, G. C., & Mathis, J. S. 1989, ApJ, 345, 245
 Chevalier, R. A. 1986, ApJ, 308, 225
 Crotts, A. P. S. 1988, ApJ, 333, L51
 Draine, B. T. 2003, ApJ, 598, 1017
 Draine, B. T., & Lee, H. M. 1984, ApJ, 285, 89
 Dwek, E. 1983, ApJ, 274, 175
 Emmering, R. T., & Chevalier, R. A. 1989, ApJ, 338, 388
 Evans, R. 2003, IAU Circ. 8150
 Graham, J. R., et al. 1983, Nature, 304, 709
 Graham, J. R., & Meikle, W. P. S. 1986, MNRAS, 221, 789
 Hamuy, M., et al. 2001, ApJ, 558, 615
 Hendry, M. A., et al. 2005, MNRAS, 359, 906
 Henyey, L. C., & Greenstein, J. L. 1941, ApJ, 93, 70
 Laor, A., & Draine, B. T. 1993, ApJ, 402, 441
 Leonard, D. C., Kanbur, S. M., Ngeow, C. C., & Tanvir, N. R. 2003, ApJ, 594, 247
 Leonard, D. C., et al. 2002, PASP, 114, 35
 Liu, J.-F., Bregman, J. N., & Seitzer, P. 2003, ApJ, 582, 919
 Maund, J. R., & Smartt, S. J. 2005, MNRAS, 360, 288
 Panagia, N., et al. 1991, ApJ, 380, L23
 Pastorello, A., et al. 2004, MNRAS, 347, 74
 Patat, F. 2005, MNRAS, 357, 1161
 Schaefer, B. E. 1987, ApJ, 323, L47
 Schlegel, D. J., Finkbeiner, D. P., & Davis, M. 1998, ApJ, 500, 525
 Schmidt, B. P., et al. 1994, ApJ, 434, L19
 Sirianni, M., et al. 2005, PASP, in press
 Smartt, S. J., et al. 2004, Science, 303, 499
 Sparks, W. B. 1994, ApJ, 433, 19
 Sparks, W. B. 1996, ApJ, 470, 195
 Sparks, W. B., et al. 1999, ApJ, 523, 585
 Sugerman, B. E. K. 2003, AJ, 126, 1939
 Sugerman, B. E. K. 2005, ApJ, in press
 Sugerman, B. E. K., & Crotts, A. P. S. 2002, ApJ, 581, L97
 Turatto, M., et al. 1998, ApJ, 498, L129
 Van Dyk, S. D., Li, W., & Filippenko, A. V. 2003, PASP, 115, 1289
 Weingartner, J. C., & Draine, B. T. 2001, ApJ, 548, 296
 Woosley, S. E., & Weaver, T. A. 1986, ARA&A, 24, 205
 Zampieri, L., et al. 2003, MNRAS, 338, 711

TABLE 1
 PHOTOMETRY OF SN 2003GD IN M74

UT date	Julian Date	<i>B</i> (mag)	<i>V</i> (mag)	<i>R</i> (mag)	<i>I</i> (mag)
2003 Aug 01 ^a	2452853.46	19.17(03)	17.41(03)
2003 Aug 25	2452876.96	19.16(08)	17.70(04)	16.61(02)	16.06(03)
2003 Aug 31	2452882.97	19.08(12)	17.66(03)	16.58(02)	16.02(03)
2003 Sep 06	2452888.96	...	17.68(04)	16.62(02)	16.08(02)
2004 Dec 8 ^b	2453347.95	23.73(08)	...	22.90(05)	...

See Van Dyk et al. (2003) for previous photometric measurements. Note: uncertainties in hundredths of a magnitude are indicated in parentheses.

^aTransformed using the prescription in Sirianni et al. (2005) from aperture magnitudes ($0''.5$ radius aperture) measured from the ACS/HRC images obtained by program GO-9733. The F435W magnitude = 19.23(01), and the F555W magnitude = 17.56(01). The F814W image of the SN is completely saturated and therefore useless.

^bTransformed using the prescription in Sirianni et al. (2005) from PSF-fitting photometry measured from our Snapshot ACS/HRC images (see text). The F435W magnitude = 23.76(07), and the F625W magnitude = 22.96(05).

TABLE 2
OBSERVED AND MODEL FLUXES FOR THE SN 2003GD LIGHT ECHO

	$F_{\text{echo}}(B)$	$F_{\text{echo}}(R)$
Observed	11 ± 7	4.9 ± 2.8
Model ^a with $d = 7.2$ Mpc ^b		
C+Si dust, $R_V = 3.1$	8.5 ± 4.5	3.5 ± 1.9
Pure Si dust, $R_V = 3.1$	14 ± 7	5.1 ± 2.7
Pure C dust, $R_V = 3.1$	3.3 ± 1.8	2.0 ± 1.0
C+Si dust, $R_V = 4.0$	8.8 ± 4.6	4.4 ± 2.3
Model ^a with $d = 9.3$ Mpc ^c		
C+Si dust, $R_V = 3.1$	5.3 ± 2.8	2.2 ± 1.1
Pure Si dust, $R_V = 3.1$	8.5 ± 4.5	3.1 ± 1.6
Pure C dust, $R_V = 3.1$	2.1 ± 1.1	1.2 ± 0.6
C+Si dust, $R_V = 4.0$	5.4 ± 2.9	2.7 ± 1.4

Fluxes are in 10^{-19} erg cm⁻² s⁻¹ Å⁻¹.

^aThe standard model for dust in the Galactic diffuse ISM is for grain radii $5.0 \text{ \AA} - 2.0 \text{ \mu m}$ and $b_C = 6 \times 10^{-5}$ (see Weingartner & Draine 2001).

^bSN distance from Van Dyk et al. (2003).

^cSN distance from Hendry et al. (2005).

Fig. 1.— *HST* images obtained at late times using the ACS/HRC of the SN II-P 2003gd in M74, showing the light echo around the SN in the (a) F435W ($\sim B$) and (b) F625W ($\sim R$) passbands.

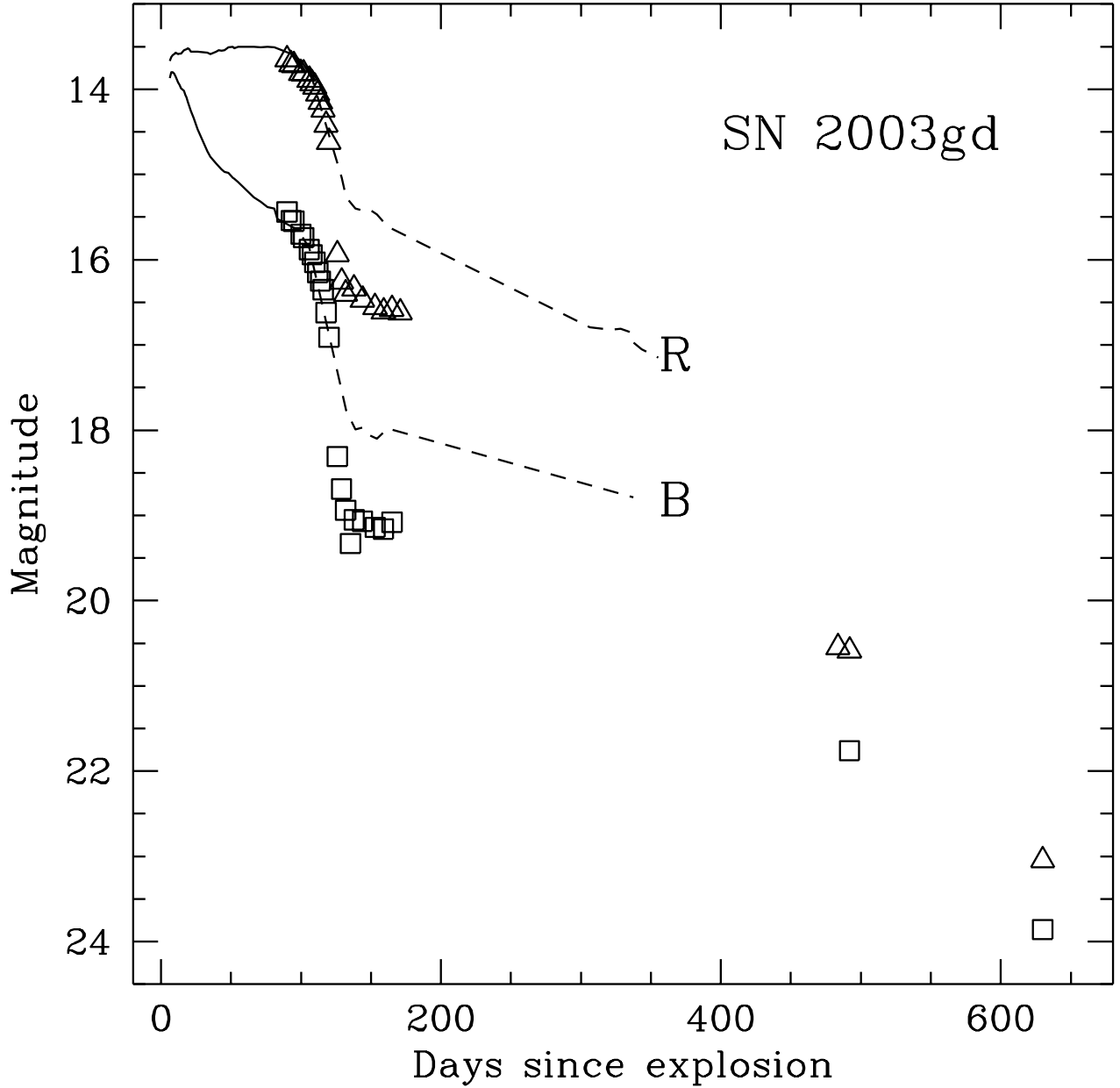


Fig. 2.— BR light curves for SN 2003gd from KAIT and *HST*/ACS observations. For comparison, the light curves for the well-studied SN II-P 1999em (Hamuy et al. 2001; Leonard et al. 2002, 2003) are shown, adjusted to the true distance modulus of M74. No additional reddening correction has been applied to the SN 1999em light curves. We extrapolate the observed SN 2003gd light curves to maximum light following the early-time SN 1999em curves (*solid lines*); the *dashed lines* represent the later-time light curves for SN 1999em.

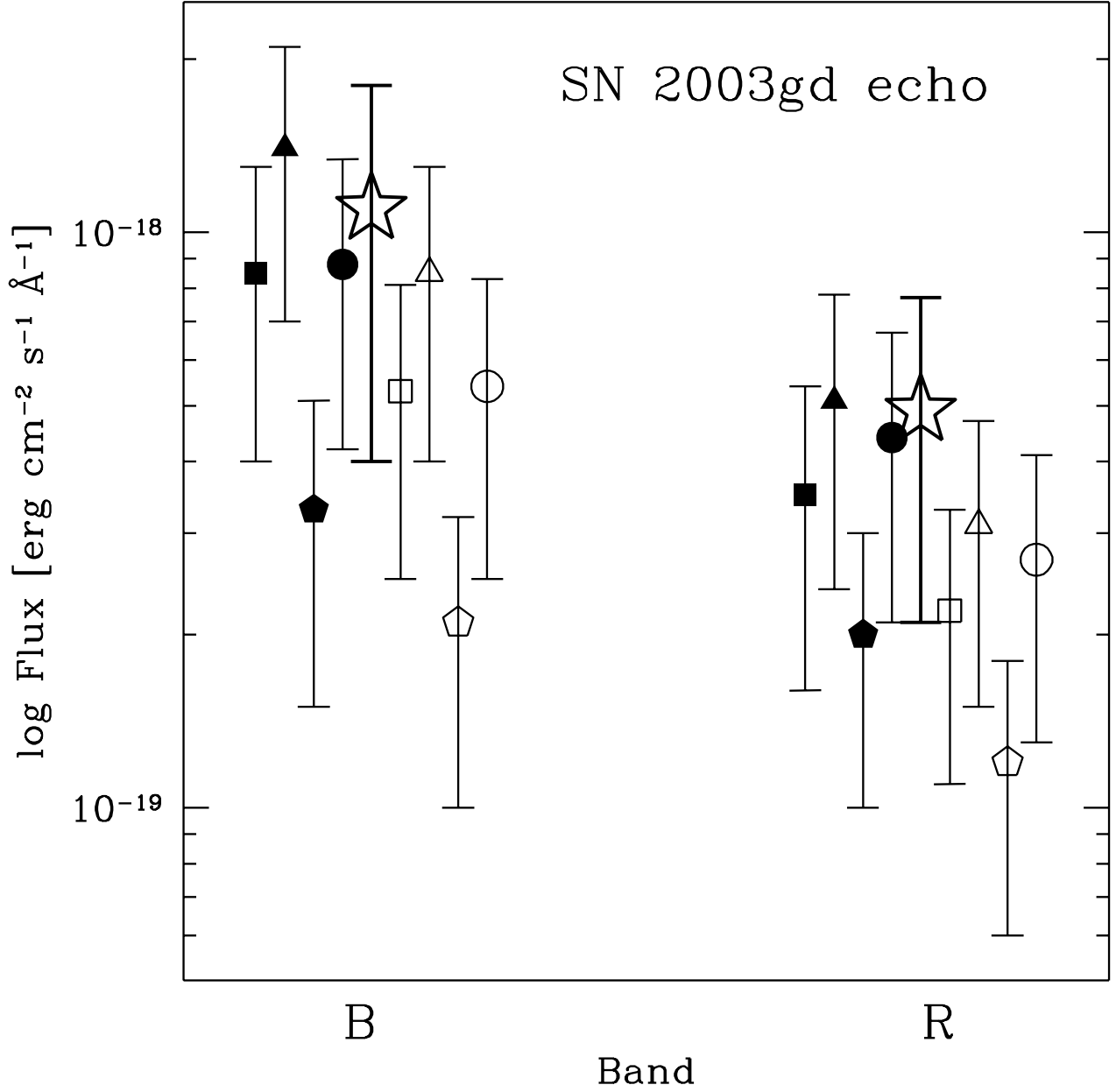


Fig. 3.— Observed and model fluxes for the echo in the B and R bands (see Table 2). The observed fluxes are represented with *stars*. The models are represented as follows for both bands: (1) For $d = 7.2$ Mpc and $R_V = 3.1$, C+Si, *filled squares*; pure Si, *filled triangles*; pure C, *filled pentagons*; and, $R_V = 4.0$ and C+Si, *filled circles*. (2) For $d = 9.3$ Mpc and $R_V = 3.1$, C+Si, *open squares*; pure Si, *open triangles*; pure C, *open pentagons*; and, $R_V = 4.0$ and C+Si, *open circles*. The datapoints for each band have been spread out along the abscissa for visual clarity.

This figure "fg1a.jpg" is available in "jpg" format from:

<http://arxiv.org/ps/astro-ph/0508684v2>

This figure "fg1b.jpg" is available in "jpg" format from:

<http://arxiv.org/ps/astro-ph/0508684v2>